UCSF
UC San Francisco Electronic Theses and Dissertations

Title

Imaging granzyme biochemistry in CAR T cell immunotherapy with restricted interaction peptides and PET

Permalink

https://escholarship.org/uc/item/85n5p9kt

Author

Sakhamuri, Sasank P.

Publication Date

2021

Peer reviewed|Thesis/dissertation

eScholarship.org Powered by the California Digital Library
University of California

Imaging granzyme biochemistry in CAR T cell immunotherapy with restricted interaction peptides and PET

by
Sasank Sakhamuri

THESIS
Submitted in partial satisfaction of the requirements for degree of
MASTER OF SCIENCE

in

Biomedical Imaging

in the

GRADUATE DIVISION
of the
UNIVERSITY OF CALIFORNIA, SAN FRANCISCO

Approved:

DocuSigned by:
Michael Evans
40E92A530F764EE...

Michael Evans
Chair

DocuSigned by:
Robert Flavell
DocuSigned by:
Henry VanBrocklin
DocuSigned by:
David Wilson
B27A8E2C2F884AC...

Robert Flavell
Henry VanBrocklin
David Wilson
Committee Members

Imaging granzyme biochemistry in CAR T cell immunotherapy with restricted interaction peptides and PET

Sasank Sakhamuri

ABSTRACT

Purpose: Recent clinical successes in the use of chimeric antigen receptor (CAR) T cell therapy has revolutionized cancer therapy. However, only 20% to 30% of patients achieve long term survival benefits, and distinguishing responders from non-responders early remains a challenge with conventional imaging techniques. Thus, there is an urgent need to develop new biomarkers to distinguish responsive and resistant patients, both to improve standard of care and to assess the antitumor activity of experimental immunotherapies. This study aims to determine the efficacy of a novel granzyme activated imaging probe to image treatment response to CAR T cell therapy in a mouse model.

Methods: Immunodeficient mice were obtained and inoculated subcutaneously with Raji tumors. CD8+ T cells were obtained from donor blood and transduced to express anti-CD19 receptors. CAR T cells were then expanded *in vitro* with IL-2. After tumors were palpable, mice were treated with empty or anti-CD19 CAR T cells intravenously. Mice were then injected with ^{64}Cu-GRIP B at 24 hours post CAR T cell administration. PET/CT studies were performed on a dedicated Inveon small animal scanner. Post mortem radiotracer uptake was quantified as %injected dose/g (%ID/g) values for tumor and normal tissue. Tumors from one representative animal per group was prepared for autoradiography.

Results: ROI analysis of static PET/CT images indicated that ^{64}Cu-GRIP B uptake in treated tumors rose from 0.5 to 2 hours post injection. Tumoral uptake of the probe was higher in anti-

CD19 CAR T versus vehicle treated arm at 2 hours post injection. The mean tumoral standard uptake values for anti-CD19 CAR T and vehicle arms were 1.5%ID/cc and 0.4%ID/cc, respectively. Biodistribution data demonstrated similar uptake of the ^{64}Cu-GRIP B probe between treatment arms as mean %ID/g for both arms was roughly 0.75. Digital autoradiography suggested substantially higher and localized uptake of the probe in the treatment arm compared to the vehicle arm in several mice.

Conclusions: Using ^{64}Cu-GRIP B, a peptide-based chemosensor whose biodistribution was engineered to be controlled by the proteolytic activity of secreted GZMB allows for imaging granzyme B mobilization by cytotoxic T cells in CAR T cell therapy. Further studies with larger samples sizes and standardized batches of CAR T cells will provide more conclusive results.

Table of Contents

List of Figures

1 INTRODUCTION

Chimeric antigen receptor T cells (CAR-T cells) are genetically engineered T cells designed to express receptor proteins specific to various antigens. In the clinical setting, a multitude of clinical trials are currently ongoing to develop and investigate novel CAR-T cells for cancer immunotherapy[1].

In conjunction, immune checkpoint inhibitor proteins (e.g., CTLA-4, PD1, PD-L1), have revolutionized cancer therapy and are thought to stimulate T cell responses against tumors [2, 3]. Currently, only a few percentage of patients experience significant clinical response, and thus, there is an urgent need to develop translational biomarkers to identify responsive and treatment resistant tumors early after the start of therapy[3].

New radiotracer development has predominantly focused on four broad classes of biological targets: (1) T cell effector proteins (e.g. PD-1, PD-L1, CTLA4) for which there is a drug target, (2) signature T cell surface markers (e.g. CD4, CD8, LAG3), (3) surface proteins upregulated on activated T cells (OX40, IL2RA, or secreted interferon gamma), or (4) metabolic pathways upregulated by activated T cells (e.g. nucleotide salvage pathways)[4, 5]. These biomarkers are valuable in that they measure a part of the complex process of T cell activation, but none show the T cell in the process of tumor cell killing.

T cells function through exocytosis of serine proteases termed granzymes (**Figure 1**). After forming a synapse with a cancer cell, T cells co-secrete granzyme B with the protein perforin, which forms a channel within the lipid bilayer of the cancer cell through which granzymes traffic into the cytosol. Once present in the cytosol, granzyme B cleaves several protein substrates to trigger apoptosis in the target cell.

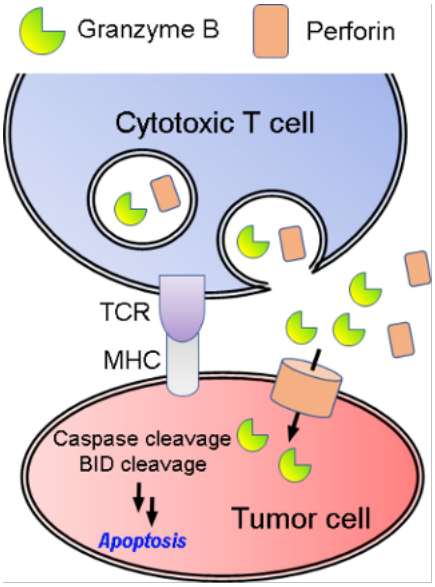

Figure 1: A schematic representation of the immunological synapse between a cytotoxic T cell and a tumor cell.

Traditional imaging probes provide a stoichiometric readout of the concentration of active enzyme molecules in a region of interest. However, these probe designs potentially inhibit the target molecule through binding to active sites, which in the case of granzyme B may partially interfere with the antitumor immune response. Thus, a protease activated nuclear imaging probe GRIP B termed a "restricted interaction peptide (RIP)" was proposed and developed at UCSF.

The RIP, GRIP B, consists of three domains from the N to C terminus (1) a non-toxic antimicrobial peptide (AMP) coupled to the radioisotope, (2) a specific endoprotease cleavage site, and (3) a peptide "masking" domain that prevents the AMP from adopting its preferred helical conformation and interacting with phospholipid membranes (**Figure 2**). Thus, upon cleavage of the full length, "propeptide" form RIP by the endoprotease of interest, the

radiolabeled AMP is liberated, spontaneously adopts a helical conformation, and inserts into any nearby membrane.

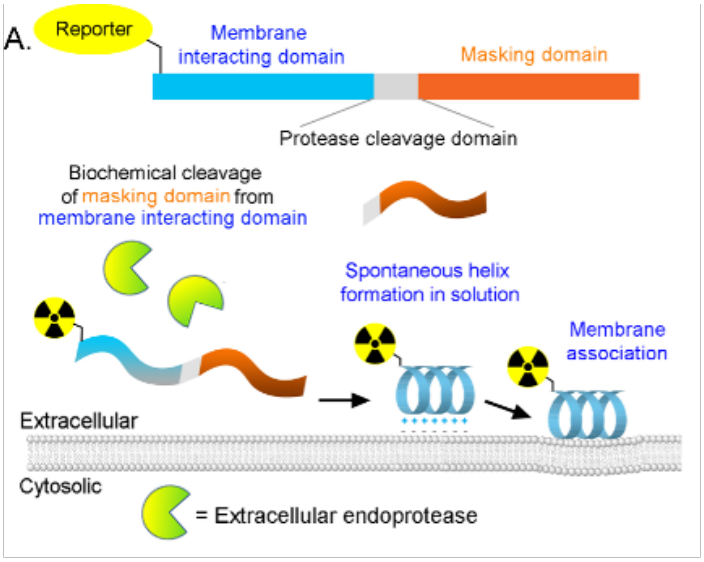

Figure 2: A schematic representation of a generic RIP, and the mechanism of action.

Currently, studies imaging T cell mobilization of granzyme B in immune checkpoint inhibitor protein therapies for several cancers in mice models are promising. Therefore, a similar study imaging granzyme B mobilization in anti-CD19 CAR T cell therapy for B cell lymphoma using a mouse model was proposed.

Preliminary Data:

To understand tracer pharmacokinetics and normal tissue biodistribution, ^{64}Cu-GRIP B uptake in C57Bl6/J mice was evaluated by conducting a 60 minute dynamic PET acquisition (**Figure 3A**). Region of interest analysis showed the probe cleared from blood pool with a $t_{1/2}$ ~8 min. The dominant mode of clearance was renal, and as with a thrombin RIP probe, the only substantial radiotracer accumulation outside of the kidneys was observed in liver.

In vivo mouse studies demonstrate that treating immunoresponsive tumors with immune checkpoint inhibitors increases ^{64}Cu-GRIP B retention in tumors. The effect of immunomodulatory therapies on ^{64}Cu-GRIP B biodistribution in mice bearing subcutaneous CT26 tumors was evaluated in a previous study, as this syngeneic mouse colorectal cancer cell line is a well-studied immunoresponsive tumor model (6). Following a schema previously reported by the Mahmood group and others, mice were treated with three i.p. infusions of vehicle or anti-PD1 combined with anti-CTLA4 therapy over 12 days (**Figure 3B**). The radiotracer was injected on day 13, and tumor uptake was monitored over several time points out to 24 hours post injection on PET. ROI analysis showed that ^{64}Cu-GRIP B uptake in the treated tumors steadily rose from 0.5 to 2-4 hours post injection (**Figure 3B**). Radioactivity persisted in tumors out to 24 hours post injection, but at a lower level compared to 4 hours. Analyzing radiotracer uptake with a dynamic PET acquisition showed rapid accumulation of ^{64}Cu-GRIP B in treated tumors, reaching a level of ~5% ID/cc within 10 min post injection. By comparison, radiotracer uptake in vehicle tumors was significantly lower and did not change over time (**Figure 3C**).

Autoradiography also underscored that ^{64}Cu-GRIP B was significantly higher in the treated tumor compared to the vehicle control, as expected (**Figure 3D**). The regions of radiotracer co-aligned with expression of granzyme B in treated tumors using IHC. A biodistribution study was conducted at 2 hours post injection to determine relative changes in tracer uptake between tissues in the vehicle and treated groups. These data showed ~50% induction of radiotracer uptake in the tumors from treated mice compared to control mice (**Figure 3E**). Remarkably, a significant increase in splenic uptake of ^{64}Cu-GRIP B uptake was

observed, which is consistent with stimulation of T cells by systemic anti-CTLA4 and anti-PD1 therapies that the Evan's lab and others have documented (7-9).

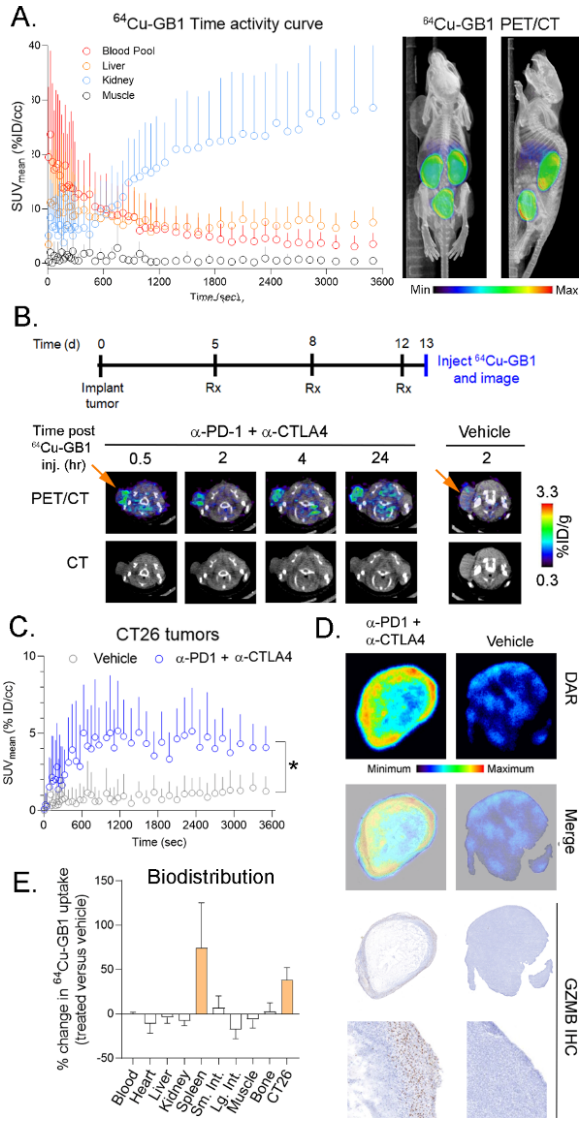

Figure 3. ^{64}Cu-GRIP B biodistribution in tumor and normal tissues. A. A time activity curve showing the biodistribution of ^{64}Cu-GRIP B in an untreated mouse bearing CT26 tumors. At right is a MIP showing the tracer accumulation from 3000-3600 sec. **B.** PET/CT images showing the uptake of ^{64}Cu-GRIP B in CT26 tumors (arrow) from mice treated with immune checkpoint inhibitors (ICIs) or vehicle. **C.** A TAC showing the tracer uptake in tumors from mice treated with ICIs or vehicle. *P<0.01. **D.** Autoradiography showing higher tracer uptake on the edge of CT26 tumors treated with ICIs. Tracer distribution co-localized with granzyme B on IHC. **E.** Biodistribution data at 2 hours post injection showing elevated tracer uptake in tumor and spleen of mice treated with ICIs versus vehicle. Tracer biodistribution in other normal tissues is comparatively less impacted by treatment. expected.

2 METHODS

2.1 General Methods:

All reagents were purchased from commercial sources and used without further purification. ^{64}Cu-chloride in hydrochloric acid was purchased from University of Wisconsin Madison. B-cell lymphoma Raji cancer cells (CCL-86 ™) were purchased from American Type Culture Collection (ATCC). Peripheral blood mononuclear cells were obtained from normal blood donors using leukoreduction filters (Vitalant Blood Services). Recombinant human GZMB was purchased from Sigma Aldrich. All cell lines were cultured according to manufacturer's instructions.

2.2 Fmoc-Solid-Phase Peptide Synthesis:

A quenched fluorogenic peptide synthesized of the sequence:

NH2-K(MCA)IEPDVSQVK(DNP)-COOH

was synthesized by Fmoc solid phase synthesis on a Biotage SyroII peptide synthesizer at ambient temperature. The synthesis scale was at 12.5 μM using preloaded lysine (2-dinitrophenyl) Wang resin where the DNP quencher was linked to the epsilon nitrogen of the lysine. Coupling reactions were carried out with 4.9 equivalents of HCTU (O-(1H-6-chlorobenzotriazole-1-yl)-1,1,3,3-tetramethyluronium hexafluoro-phosphate), 5 equivalents of Fmoc-amino acid-OH, and 20 equivalents of N-methylmorpholine (NMM) in 500 μL N,N-dimethylformamide (DMF) for 8 minutes while shaking. Each amino acid position was double coupled and subsequent Fmoc deprotection was carried out with 500 μL of 40% 4-methylpiperadine in DMF for 10-minutes followed by 6 washes with 500 μL DMF for 3-minutes. The final amino acid coupling contained the fluorophore, lysine (7-

methoxycoumarin-4-acetic acid (MCA)) where MCA was linked to the epsilon nitrogen of the lysine. Peptides were cleaved from Wang's resin with 500µL of solution composed of 95% trifluoroacetic acid, 2.5% water, and 2.5% triisopropylsilane for 1-hour while shaking. Crude peptide product was then precipitated in 30 mL cold 1:1 diethyl ether: hexanes and then solubilized in a 1:1:1 mixture of DMSO:water:acetonitrile. Solubilized crude was purified by high-performance liquid chromatography (HPLC) using an Agilent Pursuit 5 C18 column (5mm bead size, 150 x 21.2mm) on an Agilent PrepStar 218 series preparative HPLC. Mobile phase A and B were water + 0.1% TFA and acetonitrile + 0.1% TFA, respectively. Purified peptide product had solvent removed under reduced atmosphere and was solubilized into a DMSO stock with a final concentration of 10mM. Purity was confirmed by liquid chromatography-mass spectrometry and the stock was stored at -20°C.

2.3 Synthesis of DOTA-GRIP B:

DOTA-GRIP B (Dota-hexanoic acid-FVQWFSKFLGKIEPDVSQVQDPNDQYEPF-COOH) was synthesized first using standard solid phase peptide synthesis conditions as outlined above. Resin-bound peptide with N-terminal hexanoic acid was triple coupled with two equivalents of dota-NHS, five equivalents of HCTU, and twenty equivalents of N,N-Diisopropylethylamine (DIPEA) for 12-hours. DOTA-GRIP B probe was then cleaved, purified, and analyzed as described for the fluorogenic peptide.

2.4 Radiosynthesis of ^{64}Cu-GRIP B:

Into a 1.5 mL reaction vial was added 5 mCi of ^{64}Cu-chloride (aq.) and the pH was adjusted to 7.0 with Na_2CO_3 (2 M). A solution of DOTA-GRIP B (50 µg in 20 µL DMSO) and 0.1 M NH_4OAC buffer (200 µL) was added into this reaction vial. The reaction mixture was

incubated at 50 °C for 30 minutes. Reaction progress was monitored by analytical HPLC equipped with Agilent Pursuit analytical column (C18, 200 Å, 4.6 mm x 10 cm, 5 μm) or Phenomenex Luna® analytical column (C18, 100 Å, 4.6 mm x 250 cm, 10 μm) (70:30 MeOH:H_2O to 95:5 MeOH:H_2O over 10 min). The crude reaction was purified using a C18 Sep-Pak cartridge, and eluted with a small volume of CH_3CN. CH_3CN was then removed at 50 °C under vacuum and a gentle stream of N_2(g) to afford neat ^{64}Cu-GRIP B. The chelation efficacy is usually > 90% based on the HPLC. A formulation comprising 10% DMSO, 10% tween 80 and 80% saline was adopted for the further mice studies.

2.5 Anti-CD19 CAR T cells

Peripheral blood mononuclear cells were obtained from normal blood donors using leukoreduction filters. CD4+ and CD8+ T-cells were isolated via magnetic bead selection, activated with anti-CD3/CD28 beads. T cells were then lentivirally transduced with a validated anti-CD19 CAR construct, and expanded in vitro with IL-2.

2.6 Animal studies:

All animal experiments were approved by the Institutional Animal Care and Use Committee at UCSF. Four to six week old male or female NOD SCID gamma mice were purchased from Jackson Laboratory and housed with free access to the water and food. All mice were inoculated with 5×10^6 Raji tumor cells in a mixture of media and Matrigel (Corning) (v/v 1:1) subcutaneously into the left hind leg. After tumors were palpable (~200 mm^3), mice were treated with $5x10^6$ empty or anti-CD19 CAR T cells intravenously (n = 4 mice/arm). Mice were then injected with ^{64}Cu-GRIP B at 24 hours post CAR T cell administration. PET/CT studies were performed on a dedicated Inveon small animal scanner.

2.7 Biodistribution Studies:

At dedicated time points post radiotracer injection, mice were euthanized with CO_2(g) asphyxiation, and the blood was collected by direct cardiac puncture. Tissues were harvested, weighed and counted on a gamma counter (Hidex). The amount of radioactivity in the tissues was determined by comparison with a standard of known activity. The samples were decay-corrected and expressed as the percentage of the injected dose/weight of the harvested tissues (%ID/g).

2.8 Small Animal PET/CT:

^{64}Cu-GRIP B (~100 μCi/mouse) in 100−150 μL of 10% DMSO and 10% Tween 80 in saline was injected via tail vein. After a period of uptake time, mice were anesthetized with isoflurane (~2%), and imaged with a microPET/CT scanner (Inveon, Siemens). For static imaging, mice were scanned for 30 min for PET data acquisition and 10 min for CT data acquisition. For the dynamic acquisitions, the mice were anesthetized, positioned on the scanner bed, and injected intravenously with radiotracer. The dynamic acquisition was performed for 60 min followed by a 10 min CT acquisition.

List-mode PET data were histogrammed to generate sinograms that were reconstructed using a 2D ordered subsets expectation maximization algorithm provided by the scanner manufacturer. Attenuation correction was applied using the co-registered CT data that were acquired immediately following PET data acquisition. CT was acquired using the following setting: 220 degree angular coverage with 120 steps, x-ray tube operating at 80 kVp and 0.5 mA with each angular step exposure time set as 175 ms. All reconstructed 3D PET volume image

voxels were calibrated to Bq/ml using a precalibrated quantification factor. AMIDE software was used for reconstruction of PET/CT data and image analysis.

2.9 Digital Autoradiography:

Tumors or designated tissue were flash frozen in OCT in dry ice. The tissues were sectioned with a microtome (Leica) into slices with 10-20 um thickness and directly mounted on glass slides (VWR). GE Storage Phosphor Screen were exposed by such slides with radioactive tissue. After 10 half-live of copper-64, the screen was developed on a phosphorimager (Typhoon 9400). The images were further analyzed by using Fiji software.

2.10 Statistics:

All statistical analysis was performed using PRISM v8.0 or ORIGIN software. Statistically significant difference was determined by an unpaired, two-tailed Student's T test. Changes only at the 95% confidence level ($P < 0.05$) were regarded as statistically significant.

3 RESULTS

3.1 PET Imaging

We evaluated the efficacy of ^{64}Cu-GRIP B to detect granzyme B mobilization during CAR T cell therapy in mice bearing subcutaneous Raji tumors, a human B cell lymphoma cancer cell line that responds to anti-CD19 CAR T cell therapy. Mice with palpable tumors were injected with $5x10^6$ empty or anti-CD19 CAR T cells intravenously. Four mice were used in the experimental group and three mice in the control group. Mice were then injected with ^{64}Cu-GRIP B at 24 hours post CAR T cell administration. ROI analysis of static PET/CT images indicated that ^{64}Cu-GRIP B uptake in treated tumors rose from 0.5 to 2 hours post injection. Tumoral

uptake of the probe was higher in anti-CD19 CAR T versus vehicle treated arm at 2 hours post injection (**Figure 4**). The mean tumoral standard uptake values for anti-CD19 CAR T and vehicle arms were 1.5%ID/cc and 0.4%ID/cc, respectively (**Figure 4**).

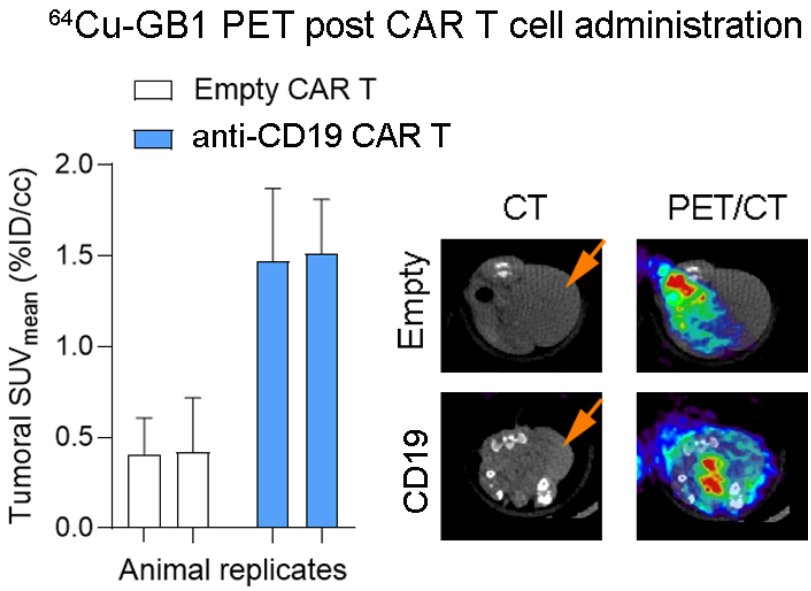

Figure 4: Uptake of ^{64}Cu-GRIP B post CAR T cell administration. Higher uptake and localization of the probe can be visualized in the anti-CD19 CAR T cell treatment arm compared to vehicle.

Radioactivity persisted in tumors out to 24 hours post injection, which is consistent with a mechanism of irreversible radiotracer trapping at the tumor. Radiotracer uptake in vehicle tumors was visually lower and did not change over time. Uptake of the probe was also visualized in the liver and spleen.

3.2 Biodistribution

After PET/CT imaging, a biodistribution study at 2 hours post injection was conducted to determine relative changes in tracer uptake between tumors in the vehicle and treated groups. This data demonstrated similar uptake of the ^{64}Cu-GRIP B probe between treatment arms as mean %ID/g for both arms was around 0.75. However, several tumors from the anti-CD19 CAR

T cell treatment arm had higher uptake values of the probe, resulting in a subset of samples in the treatment arm with higher values. (**Figure 5**).

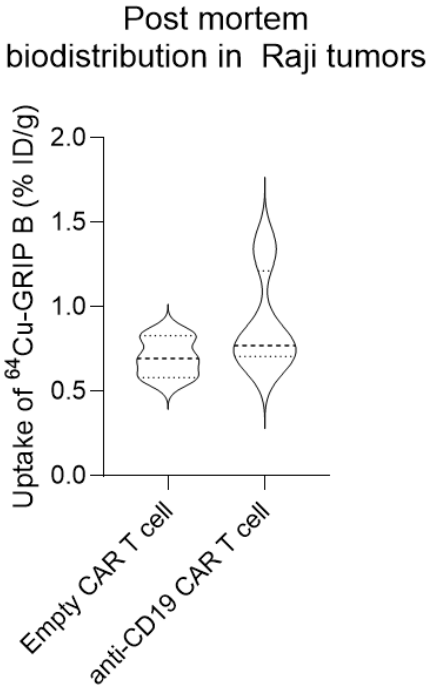

Figure 5: Violin plot of mean ^{64}Cu-GRIP B uptake post CAR T cell administration.

3.3 Digital Autoradiography

Digital autoradiography (DAR) showed that ^{64}Cu-GRIP B uptake was higher in the treated versus control tumor (**Figure 6**). Signal intensity of the ^{64}Cu-GRIP B probe was noticeably more localized and higher in several mice in the treatment arm compared to those in the vehicle arm.

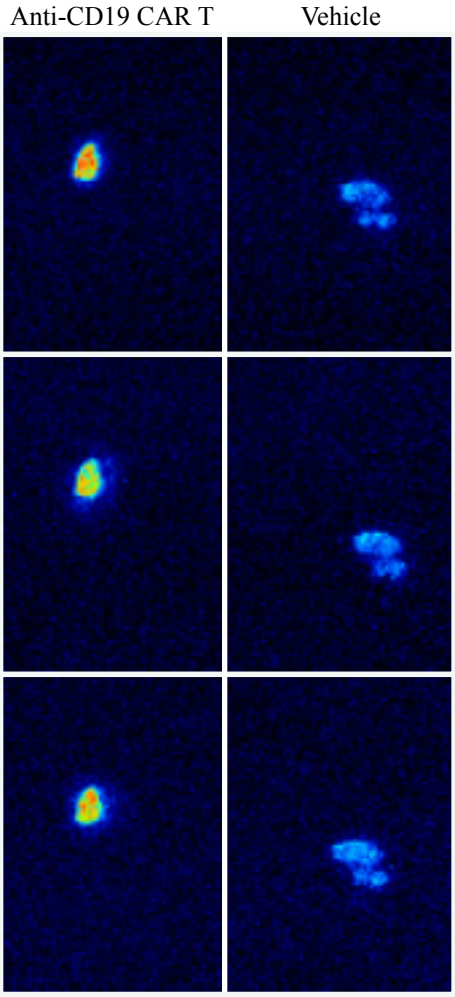

Figure 6: Autoradiography of ^{64}Cu-GRIP B uptake in sectioned tumors from treatment and vehicle arms.

4 DISCUSSION and CONCLUSION

Data from this study has demonstrated that granzyme biochemistry can be detected in vivo with nuclear imaging. Using ^{64}Cu-GRIP B, a peptide-based chemosensor whose biodistribution was engineered to be controlled by the proteolytic activity of secreted GZMB allows for imaging granzyme B mobilization by cytotoxic T cells in CAR T cell therapy. However, while many differences between treatment and control arms were visualized, these

differences were not significant. One major limitation of this study was the small number of samples per experimental arm. Several mice were required to be humanely euthanized before running the experiment due to aggressive tumor growth reaching study endpoints. Similarly, several batches of anti-CD19 CAR T cells displayed heterogeneous treatment efficacy to the known responsive tumor cell line. Difficulties that occurred during transduction and proliferation of the CAR T cells were suspected. Further studies with larger samples sizes and standardized batches of CAR T cells will provide more conclusive results.

Ultimately, observing significant differences between vehicle and anti-CD19 CAR T cell therapy, will provide subsequent grounds for correlating early changes in tumoral uptake of the GRIP B probe with long term volumetric changes in tumor and survival differences. SUVmean vs tumor volume changes will be analyzed using a Pearson correlation test. Significant differences in SUV between survivors will be assessed retrospectively after the data is collected. Also immune cell stimulation in the spleen can be a source of immune related toxicity, which underscores the potential clinical utility of globally profiling immune responses with an imaging tool like ^{64}Cu-GRIP B. Basic toxicology studies observing effects on human red blood cells were completed and no toxicity against human red blood cells in vitro was observed over 3 hours at probe concentrations up to 10 μM. Non-specific toxicity against adherent proliferating cancer cells was tested, and no significant change in cell number between vehicle and treatments up to 100 μM probe over three hours. The study results along with preliminary data are encouraging. Future control and toxicology studies in mouse models can validate the potential for use in a clinical setting.

References

1. Tsukahara T, Ohmine K, Yamamoto C, et al. CD19 target-engineered T-cells accumulate at tumor lesions in human B-cell lymphoma xenograft mouse models. *Biochem Biophys Res Commun*. 2013;438(1):84-89.
2. Leach DR, Krummel MF, and Allison JP. Enhancement of antitumor immunity by CTLA-4 blockade. *Science.* 1996;271(5256):1734-6.
3. Schumacher TN, Kesmir C, and van Buuren MM. Biomarkers in cancer immunotherapy. *Cancer Cell.* 2015;27(1):12-4.
4. Ehlerding EB, England CG, McNeel DG, and Cai W. Molecular Imaging of Immunotherapy Targets in Cancer. *J Nucl Med.* 2016;57(10):1487-92.
5. Evangelista L, de Jong M, Del Vecchio S, and Cai W. The new era of cancer immunotherapy: what can molecular imaging do to help? *Clin Transl Imaging.* 2017;5(4):299-301.
6. Lechner MG, Karimi SS, Barry-Holson K, Angell TE, Murphy KA, Church CH, et al. Immunogenicity of murine solid tumor models as a defining feature of in vivo behavior and response to immunotherapy. *J Immunother.* 2013;36(9):477-89.
7. Pai CS, Simons DM, Lu X, Evans M, Wei J, Wang YH, et al. Tumor-conditional anti-CTLA4 uncouples antitumor efficacy from immunotherapy-related toxicity. *J Clin Invest.* 2019;129(1):349-63.
8. Ise W, Kohyama M, Nutsch KM, Lee HM, Suri A, Unanue ER, et al. CTLA-4 suppresses the pathogenicity of self antigen-specific T cells by cell-intrinsic and cell-extrinsic mechanisms. *Nat Immunol.* 2010;11(2):129-35.

9. Brahmer JR, Lacchetti C, Schneider BJ, Atkins MB, Brassil KJ, Caterino JM, et al. Management of Immune-Related Adverse Events in Patients Treated With Immune Checkpoint Inhibitor Therapy: American Society of Clinical Oncology Clinical Practice Guideline. *J Clin Oncol.* 2018;36(17):1714-68.

Publishing Agreement

It is the policy of the University to encourage open access and broad distribution of all theses, dissertations, and manuscripts. The Graduate Division will facilitate the distribution of UCSF theses, dissertations, and manuscripts to the UCSF Library for open access and distribution. UCSF will make such theses, dissertations, and manuscripts accessible to the public and will take reasonable steps to preserve these works in perpetuity.

I hereby grant the non-exclusive, perpetual right to The Regents of the University of California to reproduce, publicly display, distribute, preserve, and publish copies of my thesis, dissertation, or manuscript in any form or media, now existing or later derived, including access online for teaching, research, and public service purposes.

DocuSigned by:
Sasank Sakhamuri
965AAED9E5C54EC...
Author Signature

9/2/2021
Date